1	
2	
3	
4	
5	
6	
7	
8	
9	
LO	
L1	
L2	
L3	A Tale of Two Events: Arctic Rain-on-Snow Meteorological Drivers
L4	
L5	Jessica Voveris ¹ , Mark Serreze ¹
L6	
L7	National Snow and Ice Data Center, Cooperative Institute for Research in Environmental
L8	Sciences, University of Colorado, Boulder

Abstract

- Arctic Rain on Snow (ROS) events can have significant impacts on Arctic wildlife and socioeconomic systems. This study addresses the meteorology of two different Arctic ROS events.
 The first, occurring near Nuuk, Greenland, generated significant impacts, including slush
 avalanches. The second, less severe, occurred within the community of Iqaluit, Nunavut,
 Canada. This research utilizes atmospheric reanalysis, automated surface observation station
 data, and atmospheric soundings to determine the meteorological conditions driving these
 events and the differences between them.
- 28 In both cases, atmospheric blocking played a leading role in ROS initiation, with atmospheric rivers – narrow bands of high water vapor transport, typically originating from the tropics and 29 30 subtropics – having both direct and indirect effects. Cyclone-induced low-level jets and resultant 31 "warm noses" of higher air temperatures were other key features in ROS generation. To our 32 knowledge, our study is the first to visualize how the varying strength and manifestation of these coupled features can contribute to differences in the severity of Arctic ROS events. The 33 34 meteorological drivers identified here find support from other studies of Arctic ROS events and are similar to those associated with Arctic precipitation events of extreme magnitude. 35

Introduction

36

37 Characterizing Rain-on-Snow Events and Their Impacts

- 38 Arctic rain-on-snow (ROS) events occur when liquid precipitation, in the form of rain or freezing
- rain, falls on an existing snowpack (Bieniek et al. 2018; Grenfell and Putkonen 2008; Rennert et
- 40 al. 2009; Serreze et al. 2021). In general, research on Alaskan ROS events noted that these
- conditions are most likely to occur from October through April with some studies narrowing it
- further to November through March when conditions are favorable and a snowpack is present
- (Bieniek et al. 2018; Crawford et al. 2020; Pan et al. 2018). North American and Eurasian ROS
- events may also occur during this seasonal window (Cohen, Ye, and Jones 2015).
- 45 ROS events in the middle latitudes have been studied extensively, including how their
- occurrence relates to geographic position relative to sources of maritime moisture or the number
- of rain days a location may experience (Cohen et al. 2014; Garvelmann, Pohl, and Weiler 2015;
- 48 Kattelmann 1997; McCabe, Clark, and Hay 2007). Impacts from flooding are well known,
- involving the combination of heavy rainfall and melting of the underlying snowpack (McCabe,
- 50 Clark, and Hay 2007). An area may be more susceptible to ROS-generated flooding due to
- several factors: rain over a large catchment area (which leads to a high amount of runoff), the
- 52 potential for additional snowmelt conditions and changes in snow cover dynamics (snow
- 53 metamorphism), and elevated rainfall over extended periods (when storm systems should be
- producing snow) (Garvelmann, Pohl, and Weiler 2015; Guan et al. 2016; Kattelmann 1997;
- 55 Singh et al. 1997).
- 56 ROS events can disrupt ground transportation and aviation operations, and wet-snow (or slush)
- 57 avalanches resulting from ROS can damage infrastructure (Hansen et al. 2014; Putkonen and
- 58 Roe 2003). Officials may close roads and airports due to ice formation, isolating Arctic
- 59 communities (Hansen et al. 2014). As a notable example of infrastructure impacts, a slush
- avalanche in Longyearbyen (Svalbard) destroyed a pedestrian bridge, and major roads that
- 61 serviced the community had to be closed for several days (Hansen et al. 2014). The authors
- add that Arctic locations are susceptible to wet-snow avalanches in a warming climate, as
- current infrastructure was not originally built with these natural disasters in mind.
- Following ROS occurrence, the ice layers that accumulate on, or within, the snowpack act as
- barriers to foraging, sometimes leading to mass starvation of caribou, reindeer, and musk oxen
- (Forbes et al. 2016; Rennert et al. 2009; Serreze et al. 2021). Ice formation may also force
- animals to seek other sources of food further away from their regular environments.
- 68 exacerbating the conditions leading to starvation (Serreze et al. 2021). Examples include an
- 69 Arctic ROS event that occurred on Banks Island in Canada during October of 2003 that led to
- 70 the demise of an estimated 20,000 musk oxen, an event in Svalbard in January of 2012 which
- 71 produced one of the largest numbers of reindeer carcasses found in the following summer and
- an event in the Yamal Peninsula in northern Russia during the autumn of 2013 that starved
- approximately 61,000 reindeer (out of a total of 275,000) (Forbes et al. 2016; Hansen et al.
- 74 2014; Rennert et al. 2009; Serreze, Crawford, and Barrett 2015).

75 Known Meteorology Concerning Arctic Rain-on-Snow Events

- Generally, near-surface air temperatures in the region of an Arctic ROS event increase
- dramatically preceding the onset of precipitation, typically over a relatively short time period
- 78 (Hansen et al. 2014; Rennert et al. 2009; Serreze et al. 2021). This causes rain to fall during
- part of the event (or throughout the entirety of the event) and may cause additional surface

- 80 melting. Air temperatures then decrease following the event, often to well below freezing
- 81 (Serreze et al. 2021). Liquid water freezes and forms a thick glaze of ice along the surface of
- the snow layer or within the snowpack (Serreze et al. 2021).
- This sequence of shifting temperatures frequently involves an advancing extratropical cyclone
- 84 (which generates the initial precipitation), with a cold front then progressing through the area
- (Rennert et al. 2009). Working in tandem with the overall precipitation event, increased warm air
- 86 advection with these systems causes additional melting of the surface snow layer through
- amplified mixing and turbulent fluxes (Semmens et al. 2013). For example, Rennert et al. (2009)
- 88 described a strong anticyclonic ridge at the synoptic scale that initially developed over the
- 89 Banks Island region preceding the October 2003 ROS event. This feature led to strong,
- 90 southwesterly flow bringing warmer, moister air into the area. Lift (upward motion), triggered by
- an approaching shortwave trough (extratropical cyclone), initiated precipitation across the
- region. The precipitation first began as snow then transitioned to rain as air temperatures rose
- 93 (Rennert et al. 2009).

122

- 94 Some studies have noted ROS connections with atmospheric blocking and atmospheric rivers
- 95 (ARs). Crawford et al. (2020) described a link between blocking patterns and ROS conditions in
- Alaska, in which a strong pressure gradient builds between a ridge of high-pressure and an
- 97 approaching extratropical storm system. This gradient instigates further warm air advection and
- 98 transport of positive anomalies in precipitable water, the total atmospheric water vapor
- 99 contained within an atmospheric column. Serreze et al. (2015) associated an AR with the
- January 2012 Svalbard ROS event, which coincided with an extreme event in total precipitation.
- Studies for the middle latitudes document links between ROS events in mountainous regions in
- the inland Western US and landfalling ARs along the US West Coast (Guan et al. 2016;
- 103 Trubilowicz and Moore 2017). Nevertheless, it is widely acknowledged that additional research
- is needed to understand the weather patterns influencing Arctic ROS events and how features
- like ARs and blocking setups impact their formation (Bieniek et al. 2018; Rennert et al. 2009).

Research Questions Posed for This Study

- The Arctic Rain-on-Snow Study, a team of interdisciplinary researchers and part of the National
- 108 Science Foundation's Navigating the New Arctic initiative, focuses on better understanding
- 109 Arctic ROS events and their impacts on Arctic communities. One of the project goals is to
- assess the meteorological conditions most influential in setting up ROS occurrences. As
- mentioned, Arctic ROS events occur at times of the year (October through April) when
- precipitation should usually be falling as snow and during which solar radiation is limited or even
- absent, depending on the latitude. This implies a key role of warm (and moist) air advection and
- transport from lower latitudes. As the Arctic continues to warm, one can expect both the
- seasonality and intensity of ROS events to change. This prompts three questions:
- 1. What are the primary meteorological conditions at varying spatial scales linked to Arctic ROS occurrence?
- 2. Do synoptic scale blocking patterns and atmospheric rivers play important roles in Arctic ROS initiation?
- 3. Are the strength and presence of these features (and others) influential in the severity of ROS impacts?

Case Study Selection, Data Sources, and Methodology

Selection of Case Studies

- We selected two contrasting ROS events for this study, one guite strong, the other much
- weaker. The first event occurred in Western Greenland in mid-April of 2016. A team of
- researchers confirmed it by investigating wet-snow avalanches near Nuuk, Greenland, using
- remote sensing data (Abermann et al. 2019). The authors concluded that over 800 wet-snow
- avalanches initiated during this ROS event and documented that an automated surface
- observation station was destroyed on April 11, coinciding with the day of highest air
- temperatures and precipitation rates.
- Abermann et al. (2019) briefly examined the associated weather conditions. A high-pressure
- system built over the region beginning on April 9, 2016. It continued to strengthen, progressing
- through April 10. As a warm front approached southwestern Greenland, air temperatures
- increased rapidly, and this feature provided additional moisture advection needed to produce
- significant precipitation. Abermann et al. (2019) documented that the Greenland Ecosystem
- Monitoring Program's automated meteorological station near Nuuk, Greenland, recorded this
- rapid warming (an increase of 22.2 °C from April 9-11) and a precipitation total of 25 mm during
- this same two-day period. An additional station with the Asiaq monitoring network for Nuuk
- recorded a slightly smaller temperature increase of 14.6 °C but a larger precipitation total of 49
- 140 mm for the two-day period, being a location closer to the maritime environment.
- 141 The second event occurred on January 19, 2021, in Iqaluit (Nunavut, Canada), confirmed by an
- eyewitness report on social media and relayed to the Arctic Rain on Snow Study team by one of
- its members. This case presented an opportunity to research a ROS event that had not been
- studied previously. In the lead up to this event, much of Canada had experienced a swing from
- seasonally cold to above normal air temperatures during the early part of January 2021. Around
- the beginning of the new year, atmospheric reanalysis data indicate surface air temperature
- anomalies of -5 to -20 °C across much of the Canadian Arctic. By the second week in January,
- atmospheric reanalysis showed the flip to +5 to +20 °C surface air temperature anomalies over
- the same area, likely due to the combination of a building ridge of high-pressure over western
- 150 Canada and a blocking feature over eastern Canada.
- 151 According to an article published for the Nunatsiag News on January 18, 2021, and posted on
- the Local Environmental Observer Network (a web-based platform built for community sharing
- of unusual weather events), Iqaluit was expected to continue experiencing unseasonably high
- air temperatures through the middle of the month. A low-pressure system was projected to
- move into the area through the coming week, bringing warm air from the south, and allowing air
- temperatures to remain around the freezing mark (Nunatsiaq News 2021). This was likely the
- same system that produced ROS conditions on January 19. Climate data provided by the
- Government of Canada reported that the snow depth at Iqaluit was 25 centimeters (9.84 inches)
- on January 6, 2021. There was a period of missing data from January 7 through January 19, but
- the next observation for Igaluit on January 20 indicated a snow depth of 25 cm. Therefore, we
- can safely assume that there was a snowpack at the time rain was reported on January 19.
- Documented impacts related to ROS for the 2021 Igaluit event were very limited. However, the
- effects resulting from the increased air temperatures, including on the day of the event, were
- noted. Igaluit broke its maximum air temperature record for January 19, with a new record of 0.5
- °C (CBC News 2021). According to the article from CBC News, the new temperature record
- broke the previous record of -2.2 °C, set in 1958. Subsequently, the differences in impacts
- resulting from ROS during these two events allows us to compare the meteorological features

linked to ROS occurrence and the difference in strength of these features that led to these

169 varying impacts.

170

Data Types and Acquisition

- We use ERA5 reanalysis output from the European Centre for Medium-Range Weather
- Forecasts (ECMWF). ERA5, like other reanalyses, combines observations with a dynamical
- weather model. ERA5 is known to perform well in its depiction of meteorological variables in
- 174 comparison to direct observations, including temperature, specific humidity, and wind speed
- 175 (Graham, Hudson, and Maturilli 2019). Relative to its predecessor, ERA-Interim, ERA5 also
- boasts improved depiction of synoptic- and meso-scale features, which includes cyclones, a key
- forcing for these two ROS events. Comparisons of radiosonde and PILOT data (an alternative
- upper-air balloon observation) prior to data assimilation shows an improved fit for tropospheric
- temperature, winds, and humidity (Herbach et al. 2020; Hoffmann et al. 2019). Another key
- finding from Hoffmann et al. (2019) is that ERA5 trajectories (based within Lagrangian transport
- models) better conserve stratospheric-level potential temperature, leading to smaller data
- assimilation increments that improve the uniformity of ECMWF's forecast model and
- observations. ERA5 produces hourly output at a 31-km horizontal resolution, higher than ERA-
- 184 Interim's 80-km resolution (Herbach et al. 2020).
- While ERA5 data are available hourly, we selected the 00Z (UTC) and 12Z files for this study.
- These times coincide with upper-air launch times (radiosondes), and twelve-hour increments
- still provide sufficient temporal resolution to examine the synoptic makeup of ROS events. An
- application program interface allows for different meteorological parameters to be downloaded.
- We supplemented this study with direct observations, including automated surface observation
- 190 stations and atmospheric sounding data (radiosondes). The observation network across the
- 191 Arctic remains sparse, and many of these automated sites restricted to just airports; other
- limitations include intermittent outages and upper-air data only being provided twice a day.
- Sounding data utilized with this study presents a unique dataset not analyzed in previous Arctic
- 194 ROS studies. We obtained sounding data for Aasiaat, Greenland (north of Nuuk), and for Igaluit
- 195 from the University of Wyoming sounding archive using python code provided by MetPy, a
- program developed by the University Corporation for Atmospheric Research. Automated station
- data for Godthaab (Nuuk) and Igaluit were available from the Iowa State University
- 198 (https://mesonet.agron.iastate.edu/ASOS/).

Data Visualization Methodology

- Data visualizations were divided into three atmospheric heights: upper levels, middle levels, and
- lower levels. Weather variables were chosen at these levels to best characterize various
- meteorological processes. Figure 1 provides an overview of the meteorological variables used
- in each analysis and at each atmospheric level. Additionally, MetPy code (noted above) was
- deployed in building skew-ts, commonly used to visualize sounding data. A separate python-
- 205 based program was written to provide time series data visualizations of the surface station
- 206 observations. We created these time series graphs to show the progression of temperature and
- 207 dewpoint temperature changes and precipitation type transitions, including during each ROS
- 208 event.

Upper Level Analysis	250-mb level (jet stream): geopotential heights (shows trough and ridge placement and identification of blocks)	250-mb Level
Upper Ana	500-mb level: heights and winds, including filled contours of isotachs (shows trough and ridge placement and identification of jet streaks)	500-mb Level
evel		700-mb Level
Middle Level Analysis	850-mb level: heights, winds, temperatures > 0 °C, and mixing ratio values (shows areas of warm air advection, low-level jets, and moisture transport)	850-mb Level
Lower Level Analysis	925-mb level: heights, winds, temperatures, and RH > 85% (shows areas of warm air advection, low-level jets, and moisture transport)	925-mb Level
Lower	At the surface: MSLP charts, one with PWAT and one with IVT overlaid (reveals potential moisture sources and moisture transport and atmospheric river influence)	Surface

211

212

214

215216

217218

219

220221

210 Figure 1. Weather variables examined with the reanalysis data.

Results

April 2016 Western Greenland Rain-on-Snow Event

213 Atmospheric Reanalysis

As introduced earlier, the April 2016 Western Greenland ROS event generated numerous wetsnow avalanches near Nuuk (Abermann et al. 2019). Several features stand out in the ERA5 data. In the upper levels (**Figure 2**), an Omega Block is prominent at both the jet stream level (250-mb level) and the 500-mb level. An Omega Block resembles a capital Greek letter Omega through the shape of the tropospheric, synoptic scale waveform. In this case, the ridge extending across Greenland is sandwiched between a broad trough across eastern Canada and a cutoff low over western Europe. It represents a block because of the predominant meridional flow and the persistent disruption to the general west-to-east progression of weather systems.

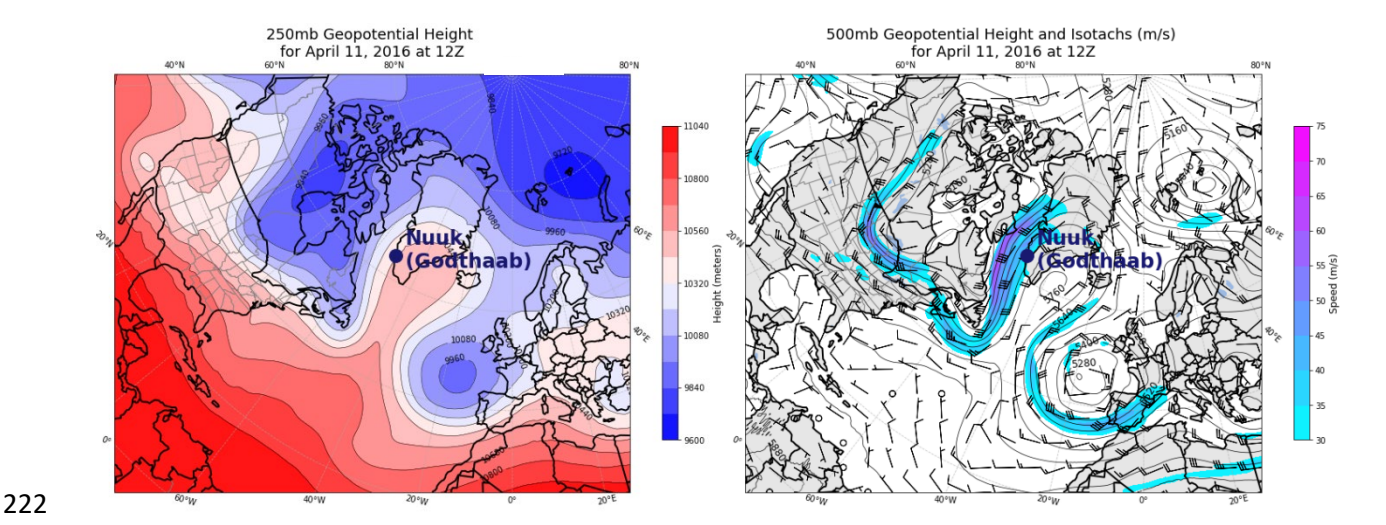


Figure 2. The 2016 Western Greenland case upper atmospheric levels. The 250-mb geopotential heights are plotted on the left, and the 500-mb heights and winds are plotted on the right. The 500-mb panel also includes isotachs (lines of constant wind speed) in m si in filled contours, in addition to wind barbs that indicate both direction and speed.

224

225 226

227

228 229

230

231

232 233

234 235

236

237

238 239

240 241

242

243 244

245

246

247 248

249

250 251

252

253

Strong wind speeds (above 50 m s. over Baffin Bay) are present at the 500-mb level along the gradient between the ridge over southern Greenland and the broad trough over eastern Canada. This area of higher wind speeds represents a jet streak. The location of interest – in this case Nuuk (Godthaab), Greenland – falls within this area that would likely be experiencing greater precipitation rates due to the additional jet dynamics. In addition, these winds are predominantly out of the south on the left (western) side of the ridge, as seen in the flag direction of the wind barbs in the 500-mb analysis. This implies a warmer air mass moving into the region. An opposing northerly flow follows on the right (eastern) side of the ridge, which likely assisted in maintaining the block.

Precipitation associated with this event can be linked to the approaching shortwave trough extending over much of the province of Quebec (Figure 2). ERA5 fields show dynamically induced rising motion on April 11, 2016, coinciding with precipitation over much of the area near Nuuk. Nuuk lies within a fjord, with surrounding terrain approaching 1000 meters. While suggesting that orographic lifting contributed to the elevated precipitation amounts, our interpretation is that dynamic lift was the dominant precipitation forcing.

In the mid- to low-levels, strong moisture transport and warm air advection accompany a cyclone-induced low-level jet (Figure 3). These features are usually associated with the precold frontal sector of an extratropical cyclone (Ralph, Neiman, and Rotunno 2005). They can be important factors in determining what locations experience precipitation and how much of it. The cited study also notes that "the low-level jet is an integral part of extratropical cyclones and is characterized by warm temperatures, weak stratification, large water vapor content, and strong low-altitude winds [Browning and Pardoe (1973), as referenced in Ralph, Neiman, and Rotunno (2005)]. Most studies agree that low-level jets may be found at an altitude of around 1 km, but wind speeds may range from 23 m s⁻¹ to 35 m s⁻¹ (Lackmann 2002; Ralph, Neiman, and Rotunno 2005). However, in Arctic locations, weaker low-level jets may be just as impactful. For example, an event near Barrow, Alaska, associated with a low-level jet of only 16 m ssufficiently warmed and moistened the boundary layer (Intrieri et al. 2014).

While the 850-mb and 925-mb analyses in **Figure 3** show the zones of higher air temperatures and moisture content, they also depict areas of warm air advection, moisture transport, and the important low-level jet. These analyses reveal how the low-level jet links to these narrow corridors of enhanced water vapor transport and unusually high air temperatures, with higher wind speeds in line with these zones. The warm air and moisture advection is clearly linked to the largely southerly flow (winds blowing from south to north) across much of southern Greenland. The height equivalent of the 850-mb level ranges from 1000 to 1500 meters and from 400 to 800 meters at the 925-mb level.

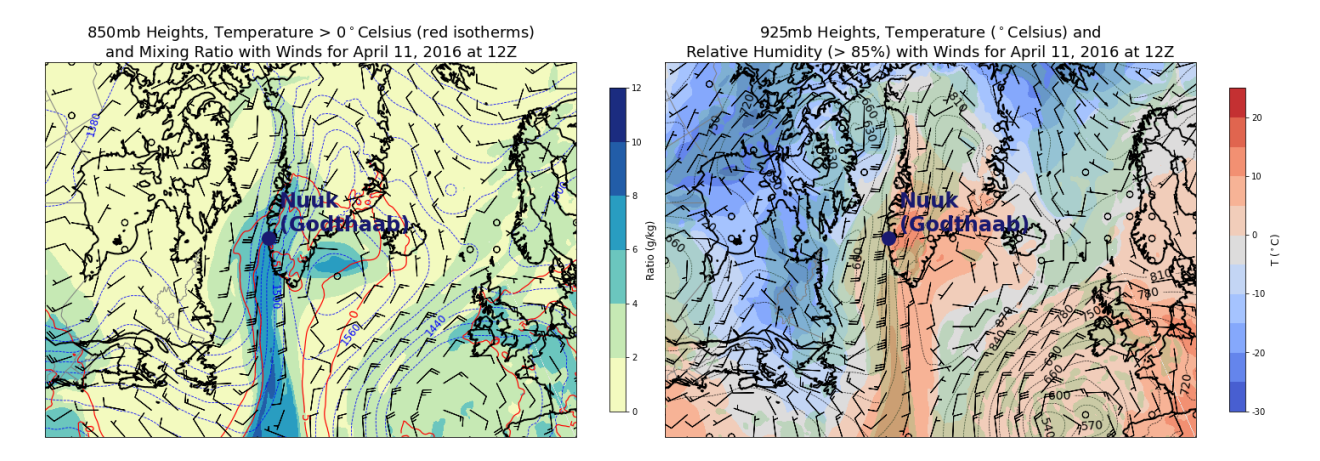


Figure 3. The 2016 Western Greenland case middle to lower atmospheric levels. The 850-mb geopotential heights are plotted on the left (which also includes mixing ratio values, winds, and air temperatures above 0 °C). The 925-mb heights, winds, air temperatures, and relative humidity above 85 percent (filled green contour) are plotted on the right.

The 2016 Greenland ROS case provides an impressive example of a corridor of high air temperatures and a narrow area of elevated moisture associated with a low-level jet. ERA5 fields for April 11 show air temperatures greater than 5 °C at 850 mb and as high as 10-15 °C across southern Greenland nearer the surface at 925 mb. **Figure 4** also shows precipitable water values of 12-16 mm over much of the southwest coast of Greenland, peaking in some locations at 20-24 mm on April 11. Climatological values of precipitable water in this area on April 11 average between 2-7 mm from the southwest coastline and extending inland. Wind speeds reach an impressive 40 m s⁻¹ at some locations along the southwest coastline in the low-to mid-levels of the atmosphere. The strong low-level jet, the position of moisture sources (North Atlantic), and the overall blocking setup appear to have worked in combination to produce this ROS event.

An extended area of elevated values of vertically integrated water vapor transport is also captured in **Figure 4**, with maximum values between 800-1000 kg m⁻ⁱs⁻ⁱ just off the southwest coast of Greenland. Based on previous AR studies, the presence of a vapor transport contour of 250 kg m⁻ⁱs⁻ⁱ stretching over 2000 km – usually from a subtropical source south of (or near) 30 °N latitude – typically meets the AR classification (Ralph et al. 2017; Rutz, Steenburgh, and Ralph 2014; Zhou et al. 2021). Additionally, the Ralph et al. (2005) study shows that the combination of strong winds associated with a low-level jet (as evidenced in **Figure 3**), as well as the high water vapor content and transport, generally create an environment suitable for AR initiation. Subsequently, this represents a case where an AR made direct landfall at the location of interest. The AR likely contributed to the increased warm air advection and moisture transport necessary for this ROS event and played a role in the extreme precipitation conditions

experienced in southwest Greenland. Comparing **Figure 4** to **Figure 2**, the blocking pattern likely had an influence on this AR setup, allowing for a large enough gradient to form between the ridge and westernmost low-pressure system.

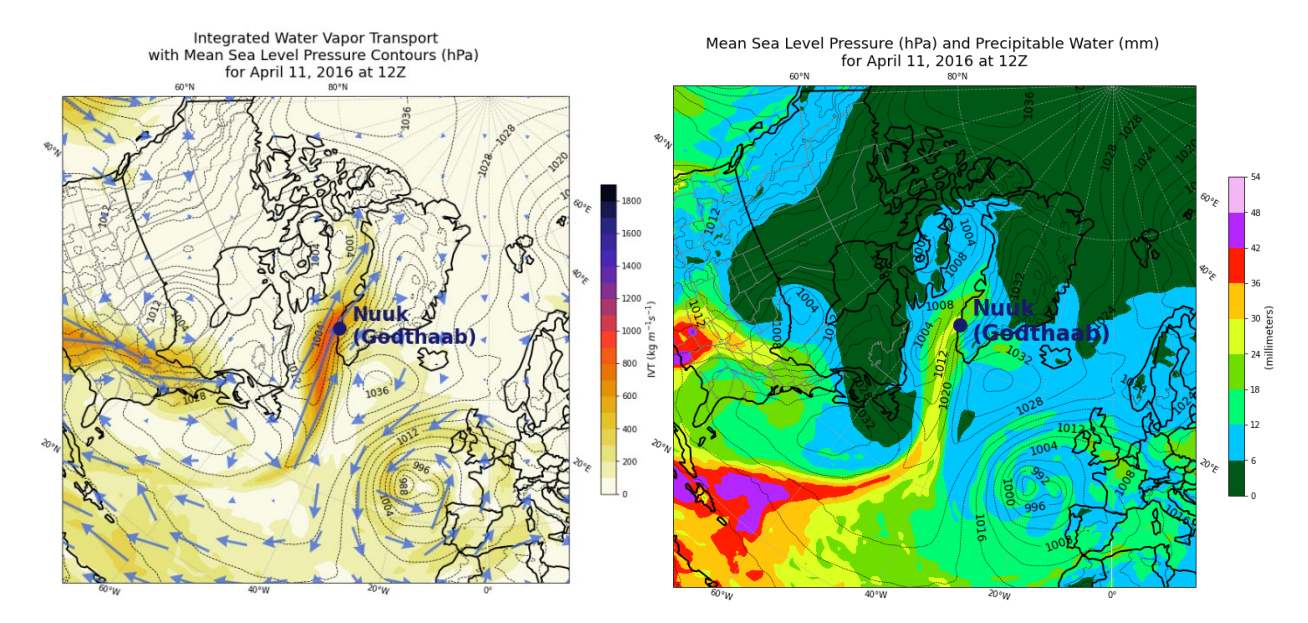


Figure 4. The 2016 Western Greenland case moisture variables. Integrated water vapor transport, with mean sea level pressure as black contours, is plotted on the left, and precipitable water, with similar mean sea level pressure contours, is plotted on the right. The vapor transport visualization includes magnitudes as filled contours, and vector arrows provide the direction.

Atmospheric Soundings

The sounding for April 11 at 12Z (top panel of **Figure 5**) captures the high moisture content and high air temperatures in the lower atmospheric levels with the 2016 Greenland ROS event. Recall that April 11 had the highest recorded wet-snow avalanche activity for this ROS event. Note the strength of the "warm nose" with this sounding. An air temperature inversion extends from the surface to about the 950-mb level, with air temperatures reaching just above 5 °C between the surface and the 900-mb level. This low-level inversion is what gives it the name "warm nose." The low-level jet, with winds above 26 m s⁻¹ in the middle to low levels of the atmosphere, is one of the more pronounced meteorological features in this case. The strength of the low-level jet (with wind directions largely out of the south, southwest) likely assisted in enhanced warm air advection and moisture transport. In addition, the precipitable water value of 19.6 mm calculated from this sounding is well above average for this time of year.

The lower sounding panel of **Figure 5** reveals how the atmospheric profile evolved in the days following the ROS event. This sounding from April 16 (five days later) is comparatively drier, with a precipitable water of 4.0 mm. A different air mass moved into the region following the passage of a likely cold front and brought much lower temperatures and the drier conditions. Air temperatures are below freezing through the entire atmospheric profile. Also noticeable are the changes in both the wind directions and speeds. Where the low-level jet was prominent in the sounding taken on April 11, with largely southwesterly winds, the sounding on April 16 shows light wind speeds around 10-15 m s⁻¹ throughout the entire column and a northwesterly direction above the mid-levels.

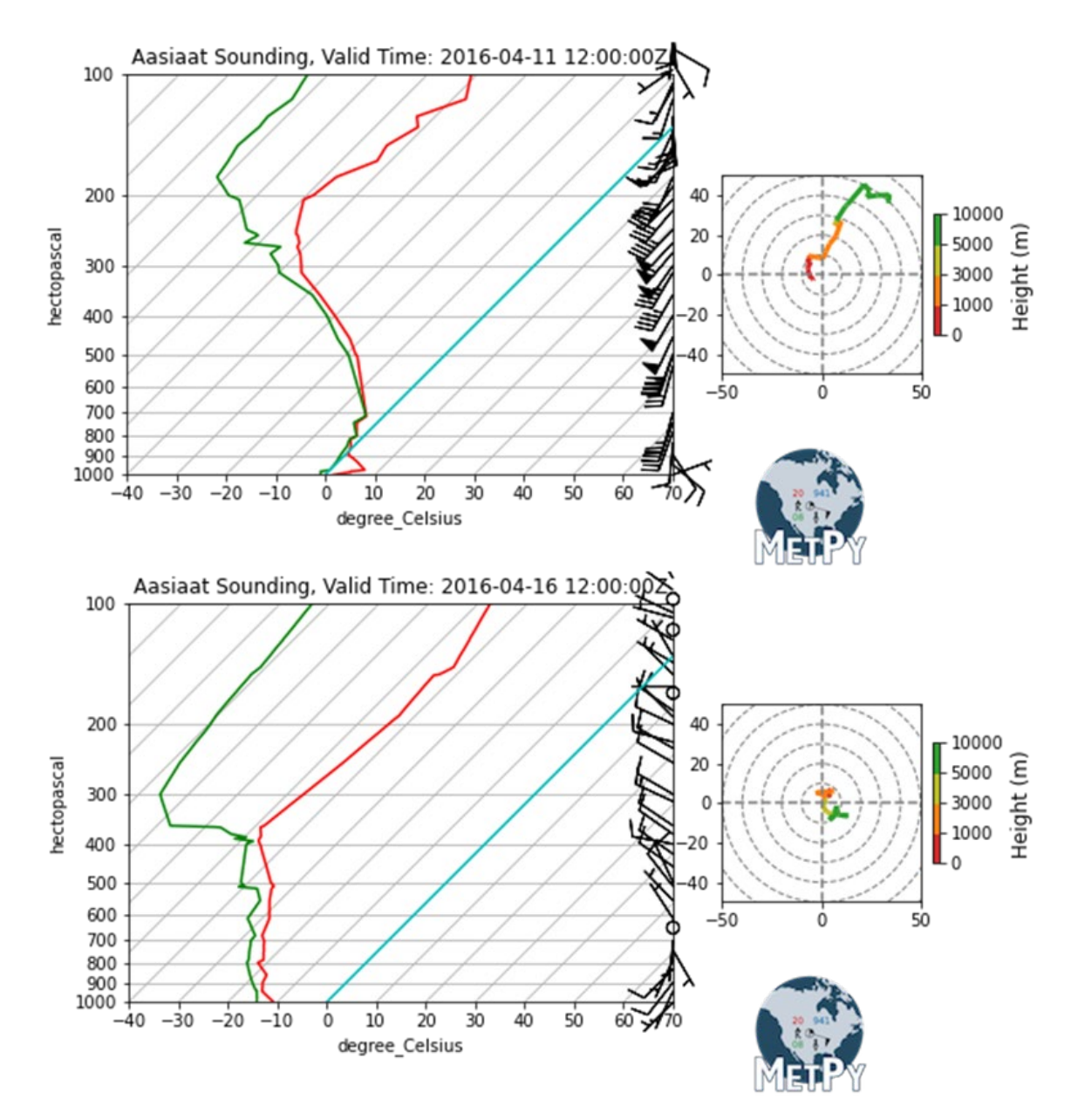


Figure 5. Aasiaat, Greenland (north of Nuuk), during and post rain-on-snow event soundings. The top sounding shows the atmospheric conditions on April 11, 2016. The bottom sounding shows the atmospheric conditions five days later. The red and green lines represent air temperature and dewpoint temperature plotted with height, respectively, and winds are plotted as both barbs on the sounding's right and as a hodograph on the right-hand side of the figure.

Automatic Surface Observing Stations

Surface observations from the Godthaab station (**Figure 6**) revealed a pattern of rising air temperatures prior to the ROS event with a corresponding change to liquid precipitation. Like the Abermann et al. (2019) analysis presented earlier, the surface air temperature increased by almost 20 °C in a two-day period from 9 to 11 April, coinciding with a liquid precipitation event. The surface station data showed the temperature rising from -2 °C at 1050Z on April 9 to its

highest temperature recorded during the period (17 $^{\circ}$ C) at the same time on April 11, a highly anomalous value for Greenland in April.

Temperatures then decreased in the following days, with air temperatures dropping below freezing beginning on April 13. Precipitation generally transitioned to solid categories at this point, with one brief period of liquid on April 14 and intervals of mixed precipitation scattered throughout. Air temperatures then remained mostly below freezing following on April 15. This would have allowed the previous liquid that fell with the initial storm system to freeze on or within the snowpack.

Godthaab, Greenland, Station Observations from April 9-17, 2016

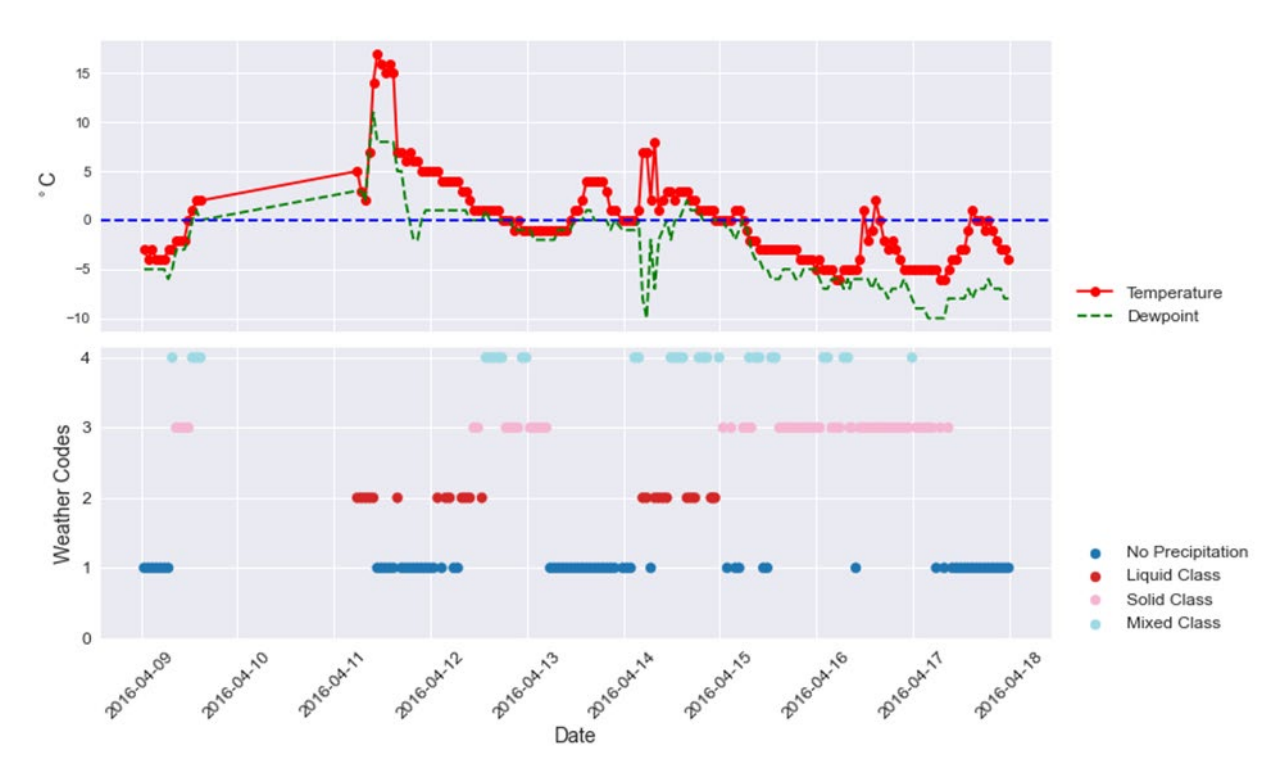


Figure 6. Godthaab (Nuuk) Greenland, surface station observations (April 9-17, 2016). Temperature and dewpoint temperature are plotted in the upper panel in °C, and the corresponding precipitation types are plotted in the lower panel.

January 2021 Iqaluit, Canada, Rain-on-Snow Event

Atmospheric Reanalysis

The Arctic Rain-on-Snow Study team was made aware of ROS conditions occurring in Iqaluit, Canada, on January 19, 2021, through an eyewitness. The weaker Iqaluit ROS case exhibited some similarities with the 2016 Greenland case, as well as notable differences. As seen in the left-hand panel of **Figure 7**, an upper-level block was present, but it was more representative of a Rex Block or Dipole Block, as opposed to the Omega Block seen in the 2016 Greenland case. Rex Blocks form when a trough undercuts a ridge, so the synoptic pattern appears as a ridge positioned poleward over a trough.

The right-hand panel of **Figure 7** shows a strong jet streak at 500 mb (with wind speeds exceeding 55 m s⁻¹) on the equatorward side of a deep trough extending across eastern Canada – likely assisting in maintaining the overall block by undercutting the ridge. Another weaker jet streak (with winds between 30 and 35 m s⁻¹) is located on the western, or left, side of the ridge of high-pressure positioned over southern Greenland. This implies additional dynamics influencing precipitation over the southern tip of Baffin Island. Even though the winds in this jet streak were largely from the south, like the Greenland case, speeds were not as strong. However, it did represent another instance of the location of interest positioned directly beneath the southerly flow aloft.

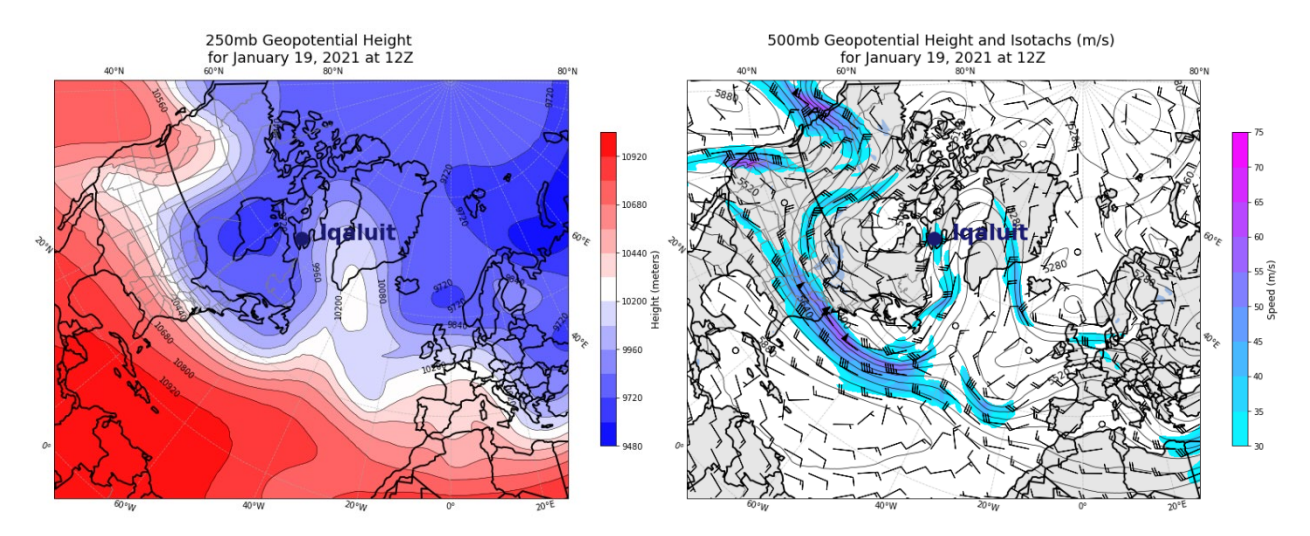


Figure 7. The 2021 Iqaluit case upper atmospheric levels. The 250-mb geopotential heights are plotted on the left, and the 500-mb heights and winds are plotted on the right. The 500-mb panel also includes isotachs (lines of constant wind speed) in m s⁻ in filled contours, in addition to wind barbs that indicate both direction and speed.

Precipitation produced during the 2021 Iqaluit event, also like the 2016 Greenland event, is largely dynamically driven. As with the Greenland event, a shortwave trough (**Figure 7**) progressing north towards Baffin Island on January 19 provides the rising motion necessary for precipitation generation. Iqaluit lies in an inlet linked to Frobisher Bay, and the surrounding terrain lies between 500 and 1000 meters. Hence, orographic lifting may have also been a contributing factor, as we also surmise for the 2016 Greenland ROS event.

Like the 2016 Greenland ROS case, the 2021 Iqaluit event is linked to narrow corridors of strong moisture transport and warm air advection. However, air temperatures with this case remained just below freezing in the middle to lower levels, and precipitable water values were lower. **Figure 8** shows air temperatures at the 925-mb level (right-hand panel) in the 0 to -8 °C range over Iqaluit. The only area with air temperatures above freezing at this level is over southern Greenland, which also extends to the 850-mb level (left-hand panel). Mixing ratios are also lower compared to the Greenland case. However, precipitable water values (while modest) are above average, ranging from 8-12 mm across the southern tip of Baffin Island (right-hand panel of **Figure 9**). Climatological precipitable water values for January 19 span from 1-4 mm across southern Baffin Island.

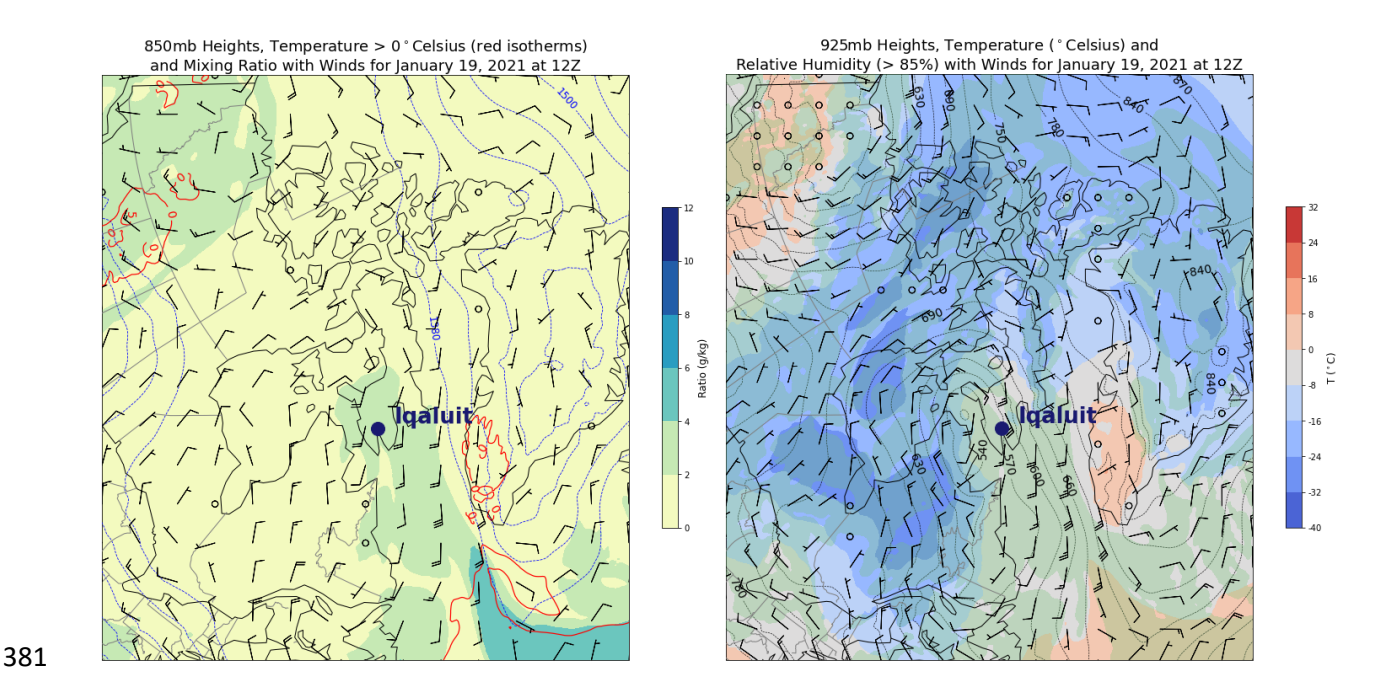


Figure 8: The 2021 Iqaluit case middle to lower atmospheric levels. The 850-mb geopotential heights are plotted on the left (which also includes mixing ratio values, winds, and air temperatures above 0 °C). 925-mb heights, winds, air temperatures, and relative humidity above 85 percent (filled green contour) are plotted on the right.

Southerly winds persist throughout the troposphere over Iqaluit, also like the Greenland case. The Iqaluit event also exhibits a cyclone-induced low-level jet but with weaker speeds compared to the Greenland case. Wind speeds are around 20 m s⁻¹ in the 850-mb analysis and around 30 m s⁻¹ at 925 mb (**Figure 8**). These lower-level winds are associated with the warm sector of a cyclone centered near the northern tip of Quebec.

A comparatively large difference with this case is the AR influence. Where the direct impact of a landfalling AR was associated with the ROS event in Greenland, the Iqaluit ROS event appears to have been indirectly influenced by an AR. The same cyclone that produces precipitation in the Iqaluit region likely stripped moisture from the AR present in the North Atlantic as it rounded the broad low-pressure area over eastern Canada (left-hand panel of **Figure 9**). The right-hand panel of **Figure 9** shows a similar pattern in precipitable water, with higher values (up to 42 mm) reflecting the position of the AR and a narrow corridor of 12-18 mm flowing north towards Baffin Island.

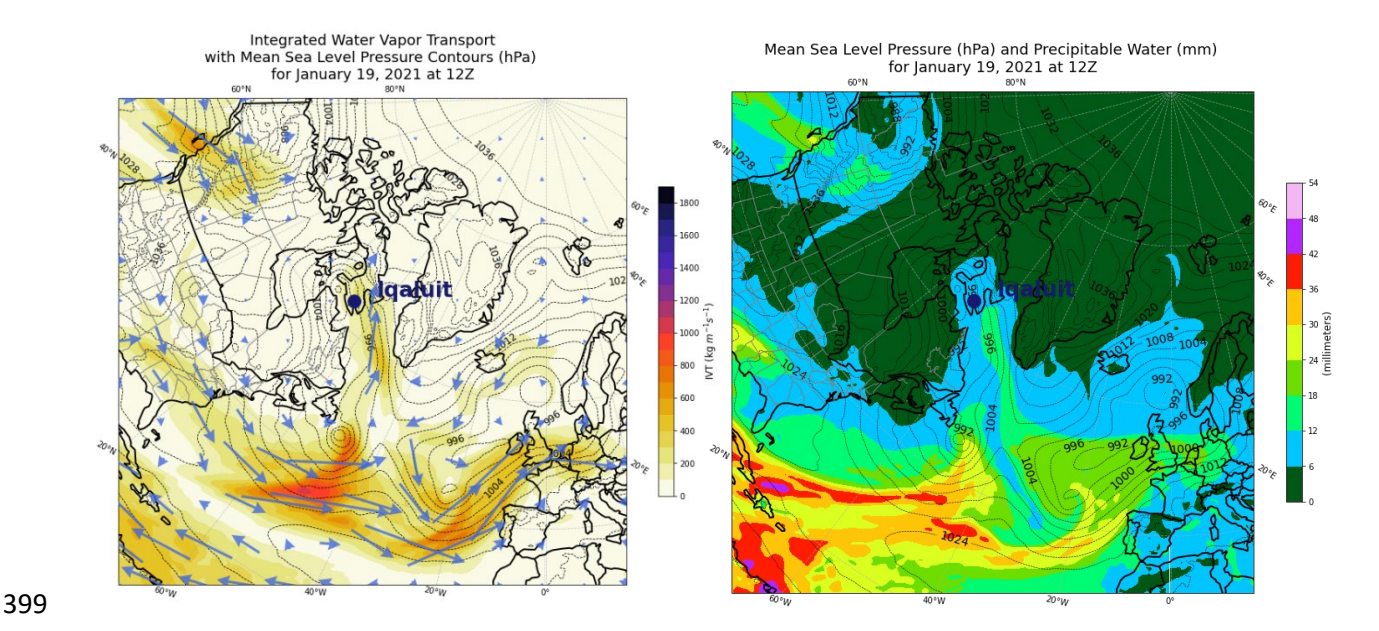


Figure 9. The 2021 Iqaluit case moisture variables. Integrated water vapor transport, with mean sea level pressure as black contours, is plotted on the left, and precipitable water, with similar mean sea level pressure contours, is plotted on the right. The vapor transport visualization includes magnitudes as filled contours, and vector arrows provide the direction.

Atmospheric Soundings

Atmospheric soundings for the 2021 Iqaluit case also highlight significant differences compared to the Greenland case. As seen in the top panel of **Figure 10**, the warm layer is very much limited to the surface on January 19 with no prominent "warm nose." We also saw this in the earlier 925-mb air temperatures in the reanalysis, with no areas exhibiting above freezing conditions. In an extensive study of relationships between sounding profiles and precipitation types, Rauber et al. (2000) found that for a majority of soundings with no warm layers – such as this example from the Iqaluit case – freezing drizzle was reported.

The Iqaluit sounding from January 19 yields a precipitable water value of 9.2 mm, high for the region and time of year, but modest compared to the 2016 Greenland case. The January 19 sounding also confirms a low-level jet with this case, with wind speeds of 21-26 m s⁻¹ between 1 and 2 km above ground level. There is evidence of veering (turning clockwise with height) winds, indicating warm air advection. Direct onshore flow, with winds out of the southeast, is similar to the 2016 Greenland case and provides the additional moisture transport for precipitation.

The sounding for January 25, six days after the ROS event, shows how the atmospheric profile changed when a new air mass moved in and geopotential heights lowered aloft (bottom panel of **Figure 10**). Temperatures fell, especially after the passage of the cold front. The moisture profile also became much drier. This sounding's precipitable water fell to 4.3 millimeters (closer to climatological values) from the 9.2 millimeters computed from the January 19 sounding. Wind behavior also changed drastically. Wind speeds slackened and directions appeared to back to the northeast, meaning cold air advection.

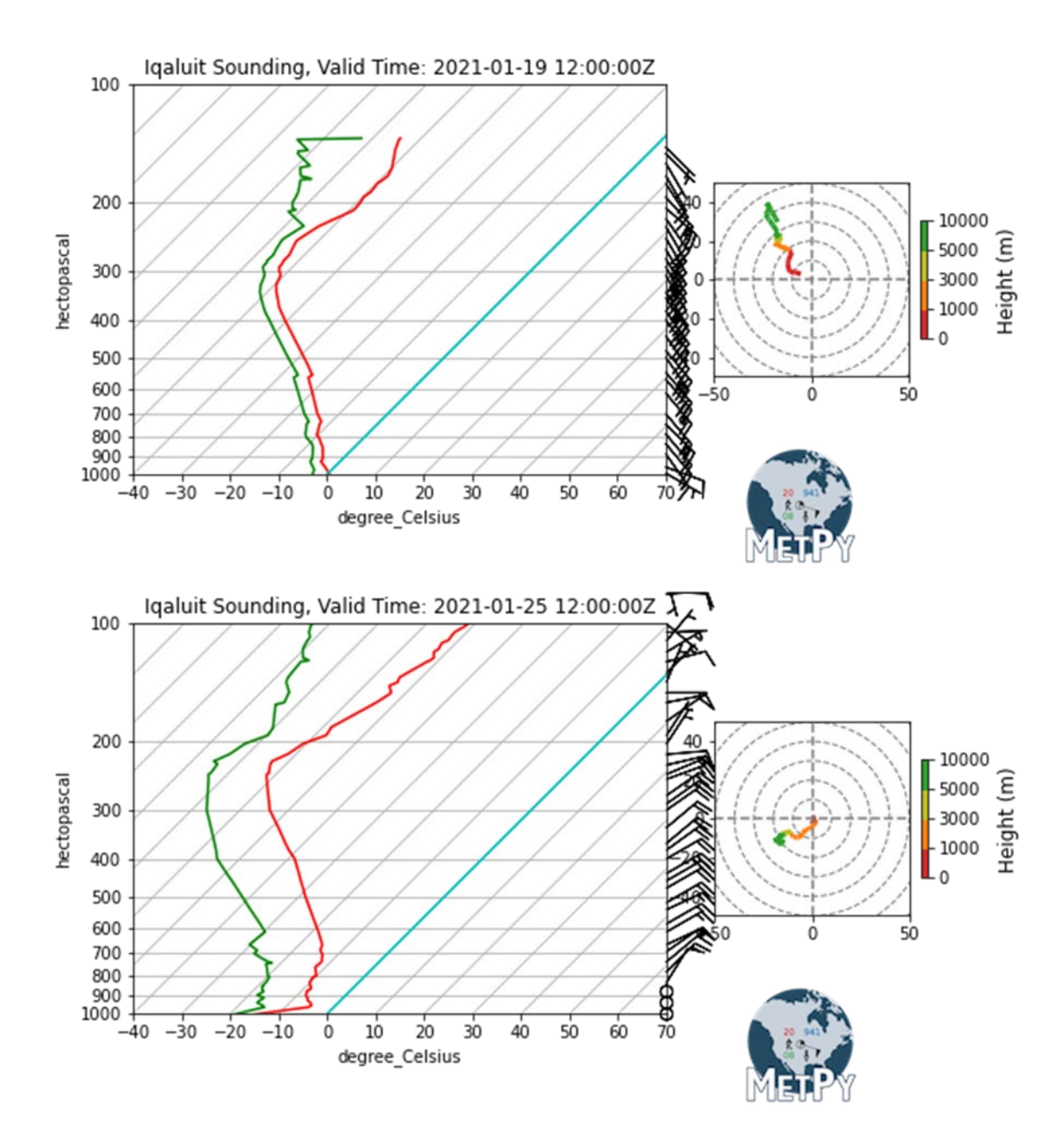


Figure 10. Iqaluit, Nunavut, during and post rain-on-snow event soundings. The top sounding shows the atmospheric conditions on January 19, 2021. The bottom sounding shows the atmospheric conditions six days later. The red and green lines represent air temperature and dewpoint temperature plotted with height, respectively, and winds are plotted as both barbs on the sounding's right and as a hodograph on the right-hand side of the figure.

Automatic Surface Observing Stations

Another interesting aspect of this case is the lack of liquid or even mixed precipitation types recorded in the automated weather station observations at the time of ROS occurrence (**Figure 11**). An eyewitness confirmed this ROS event, so this exemplifies a situation where the automated station data (usually collocated with an airport) was not representative of all regional conditions. Rauber et al. (2000) noted that soundings yielding deep cloud-top altitudes and no

warm layer throughout the atmospheric column (top panel of **Figure 10**) may produce a mix of precipitation types, like light snow, ice pellets, or freezing rain. Based on data provided by the Moderate Imaging Spectroradiometer instrument aboard the National Aeronautics and Space Administration's Aqua satellite, cloud top heights in the area were in the range of 4000 to 7000 meters during a daytime overpass on January 19, 2021. Rauber et al. (2000) noted that some of the soundings in the category exhibiting no warm layers were associated with cloud tops above 5000 meters. The authors of that paper also cautioned that surface observations and sounding data are not usually concurrent in place and time. Weather balloons tend to drift downwind from the launch site, especially in strong winds, as was likely the case here.

This was a dynamic weather event, with a relatively strong cyclone, enhanced moisture transport, and brisk winds, so it is conceivable that observations may not match actual conditions witnessed in Iqaluit. Nevertheless, the station records demonstrate the same pattern seen with the 2016 Greenland event. Surface air temperatures increased – in this case to just the freezing point on January 19 – with solid precipitation (snow) continuing. Falling air temperatures in successive days would have allowed ice to form from any liquid precipitation that accumulated on the existing snowpack. Surface air temperatures rose to the freezing point again for only a brief period on January 22 but then dropped well below freezing and remained so in the days following.





Figure 11. Surface station observations from Iqaluit (January 17-26, 2021). Temperature and dewpoint temperature are plotted in the upper panel in °C, and the corresponding precipitation types are plotted in the lower panel.

Summary and Concluding Thoughts

For the two ROS cases examined here, atmospheric blocking acted as a primary causal mechanism. This reaffirms the importance of blocks, as examined in other ROS cases (Voveris, 2022). With a block, the normal west-to-east geostrophic flow becomes disrupted – replaced by meridional flow – and provides the time for warm air masses to move in and for gradients to build for the additional moisture transport. Blocks may come in a variety of forms, and the differences between the two cases (an Omega Block for the 2016 Greenland event and a Rex Block for the 2021 Igaluit event) likely led to the difference in strength of ROS conditions. The two sites that experienced ROS were similarly situated directly beneath the strongest southerly flow aloft, between the overall ridge of high-pressure and the westernmost trough of the block. This positioned Igaluit and Nuuk under an upper-level jet streak, which generated additional jet dynamics for precipitation. Blocking patterns in these cases, and other cases examined by Voveris (2022), developed a few days prior to the day (or days) of ROS conditions and required a few days after the event to weaken and for the geostrophic flow to return to somewhat "normal" conditions.

Another key component to Arctic ROS formation was the presence of an AR and its direct or indirect influences, which reiterates findings from Voveris (2022). ARs represent a significant source of water vapor transport (and associated high air temperatures) outside of the tropics. When ARs breach the higher latitudes during the winter months, they allow warm, moist conditions to overcome the typical cold, dry Arctic environment and limited solar radiation to produce ROS. We found that the 2016 Greenland ROS event resulted from a direct AR influence (the AR making landfall), while that the 2021 Igaluit ROS event was influenced indirectly by a cyclone stripping moisture from an AR and carrying this moisture north. The direct AR landfall at Nuuk, Greenland led to a much more pronounced ROS event while the lack of a direct AR landfall at Iqaluit led to much smaller impacts.

We also document the role of cyclone-induced low-level jets and "warm noses". Soundings show how the 2016 Greenland case – directly influenced by an AR – exhibited a strong low-level jet, a deep "warm nose" layer, and a mostly saturated atmospheric column. Comparatively, the 2021 Iqaluit case was impacted by the same features but to a lesser extent. Moisture and air temperatures were lower, no "warm nose" was present, and the low-level jet was weaker, a possible consequence of only the indirect influence of an AR. These combined features were enough to adequately warm and moisten the boundary layer, leading to the report of ROS in Iqaluit, but were not enough to produce a strong ROS event as seen at Nuuk Greenland.

To our knowledge, our study is the first to show how atmospheric blocking, ARs, and other mesoscale features, such as low-level jets and subsequent "warm noses," work in tandem to produce Arctic ROS events of differing magnitude. In a recent study by Serreze et al. (2022), the key meteorological features discussed here, and noted by Voveris (2022) for other ROS events, can also be associated with Arctic precipitation events of extreme magnitude (either snow- or rain-driven). The interplay between these meteorological drivers is complex and will vary on a case-by-case basis, but some connections have been established between these features themselves and the influence they have on precipitation generation. For example, Ralph et al. (2005) note that low-level jets may coincide with AR development when combined with high water vapor content and transport. A study from Benedict et al. (2018) demonstrates how atmospheric blocking slows the normal progression of shortwave systems, shifting the storm track equatorward, while the high-pressure ridge (resulting from the blocking and developing 7-10 days prior to an AR) directs more systems toward the study area. This leads to higher chances of both AR incidence and extreme precipitation events (Benedict et al. 2018).

- Having established these meteorological links to Arctic ROS events, we can infer how future
- 508 global warming might influence ROS occurrence and intensity. Uncertainties remain regarding
- 509 how climate change will affect atmospheric blocking. Some studies argue that blocking patterns
- 510 might decrease in frequency in the middle latitudes as the climate warms or that areas that
- experience a climatologically high number of blocking episodes may see a shift in those areas
- 512 (Woollings et al. 2018). However, Woollings et al. (2018) caution that the ability of climate
- 513 models to handle blocks remains unclear and that natural variability is likely to have a strong
- 514 influence on blocking patterns in coming decades. They also add that the effect of wintertime
- 515 blocking on air temperatures is dependent upon thermal advection a process expected to
- weaken in a warming world but the effect of summertime blocking on air temperatures may
- strengthen from feedbacks resulting from changes in soil moisture.
- Results from climate model studies are in general agreement that future warming will coincide
- with increased poleward moisture transport and elevated Arctic precipitation with a transition to
- a more rain-dominated climate (Lenearts et al. 2020; McCrystall et al. 2021; Niwano et al.
- 521 2021). More rainfall implies more ROS events. However, a shorter snow cover season may lead
- to fewer ROS events, especially during the autumn or spring months, or to more incidents of
- rain falling on frozen ground instead. In addition, Espinoza et al (2018) found that climate
- models project a 10% decrease in the number of ARs, based on the "worst-case" global
- 525 emissions scenario from the Intergovernmental Panel on Climate Change. However, they note
- that models also project ARs to be 25% longer, 25% wider, and have larger integrated vapor
- transport values, likely due to the increasing moisture available in a warming atmosphere. This
- 528 implies that more ARs may potentially reach high Arctic regions, and that stronger vapor
- transport would lead to more extreme precipitation events coinciding with ROS.

Acknowledgements

530

538

- This study was supported by the National Science Foundation Grant ICER 1928230 "NNA Track
- 1: A Systematic Pan-Arctic Analysis of Rain on Snow and Extreme Precipitation Events and
- their Impacts on Human-Environment Systems." We thank Mistia Zuckerman and Tori McLeod
- for their time and effort in the final editing and submission of this manuscript. We also
- appreciate the ECMWF and UCAR for their data and MetPy programming codes (respectively)
- used in this research. We accessed ERA5 data from the Copernicus Climate Data Store API
- 537 [Application Program Interface], maintained by the ECMWF.

References

- Abermann J, Eckerstorfer M, Malnes E and Ulf Hansen B (2019) A Large Wet Snow Avalanche
- 540 Cycle in West Greenland Quantified Using Remote Sensing and in Situ Observations. *Natural*
- 541 Hazards 97 (2): 517–34. https://doi.org/10.1007/s11069-019-03655-8.
- Benedict JJ, Clement AC and Medeiros B (2019) Atmospheric Blocking and Other Large-Scale
- 543 Precursor Patterns of Landfalling Atmospheric Rivers in the North Pacific: A CESM2 Study.
- Journal of Geophysical Research: Atmospheres 124(21), 11330–11353.
- 545 doi:10.1029/2019JD030790.
- 546 Bieniek P and 6 others (2018) Assessment of Alaska Rain-on-Snow Events Using Dynamical
- 547 Downscaling. Journal of Applied Meteorology and Climatology 57 (8): 1847–63.
- 548 https://doi.org/10.1175/JAMC-D-17-0276.1.

- CBC News (2021) Iqaluit sets record high temperature for Jan. 19, reaching 0.5 C. CBC News.
- CBC. https://www.cbc.ca/news/canada/north/iqaluit-sets-record-high-temperature-for-jan-19-
- 551 reaching-0-5-c-1.5882621.
- 552 Cohen J and 6 others (2014) Recent Arctic Amplification and Extreme Mid-Latitude Weather.
- 553 Nature Geoscience 7 (9): 627–37. https://doi.org/10.1038/ngeo2234.
- 554 Cohen J, Ye H and Jones J (2015) Trends and Variability in Rain-on-Snow Events. *Geophysical*
- 555 Research Letters 42 (17): 7115–22. https://doi.org/10.1002/2015GL065320.
- 556 Crawford AD, Alley KE, Cooke AM and Serreze MC (2020) Synoptic Climatology of Rain-on-
- 557 Snow Events in Alaska. *Monthly Weather Review* 148 (3): 1275–95.
- 558 https://doi.org/10.1175/MWR-D-19-0311.1.
- Espinoza V, Waliser DE, Guan B, Lavers DA and Ralph FM (2018) Global Analysis of Climate
- Change Projection Effects on Atmospheric Rivers. *Geophysical Research Letters* 45 (9): 4299–
- 561 4308. https://doi.org/10.1029/2017GL076968.
- Forbes BC and 6 others (2016) Sea Ice, Rain-on-Snow and Tundra Reindeer Nomadism in
- Arctic Russia. *Biology Letters* 12 (11): 20160466. https://doi.org/10.1098/rsbl.2016.0466.
- Garvelmann J, Pohl S and Weiler M (2015) Spatio-Temporal Controls of Snowmelt and Runoff
- Generation during Rain-on-Snow Events in a Mid-Latitude Mountain Catchment. Hydrological
- 566 Processes 29 (17): 3649–64. https://doi.org/10.1002/hyp.10460.
- 567 Graham RM, Hudson SR and Maturilli M (2019) Improved Performance of ERA5 in Arctic
- 568 Gateway Relative to Four Global Atmospheric Reanalyses. *Geophysical Research Letters* 46
- 569 (11): 6138–47. https://doi.org/10.1029/2019GL082781.
- 570 Grenfell TC and Putkonen J (2008) A Method for the Detection of the Severe Rain-on-Snow
- 571 Event on Banks Island, October 2003, Using Passive Microwave Remote Sensing. Water
- 572 Resources Research 44 (3). https://doi.org/10.1029/2007WR005929.
- 573 Guan B, Waliser DE, Ralph FM, Fetzer EJ and Neiman PJ (2016) Hydrometeorological
- 574 Characteristics of Rain-on-Snow Events Associated with Atmospheric Rivers. *Geophysical*
- 575 Research Letters 43 (6): 2964–73. https://doi.org/10.1002/2016GL067978.
- Hansen BB and 8 others (2014) Warmer and Wetter Winters: Characteristics and Implications of
- an Extreme Weather Event in the High Arctic. *Environmental Research Letters* 9 (11): 114021.
- 578 https://doi.org/10.1088/1748-9326/9/11/114021.
- Hersbach H and 6 others (2020) The ERA5 Global Reanalysis. Quarterly Journal of the Royal
- 580 Meteorological Society 146 (730): 1999–2049. https://doi.org/10.1002/qj.3803.
- Hoffmann, L, and 10 others (2019) From ERA-Interim to ERA5: The Considerable Impact of
- 582 ECMWF's Next-Generation Reanalysis on Lagrangian Transport Simulations. *Atmospheric*
- 583 Chemistry and Physics 19: 3097–3124, https://doi.org/10.5194/acp-19-3097-2019.
- Intrieri JM and 8 others (2014) Global Hawk Dropsonde Observations of the Arctic Atmosphere
- Obtained during the Winter Storms and Pacific Atmospheric Rivers (WISPAR) Field Campaign.

- 586 Atmospheric Measurement Techniques 7 (11): 3917–26. https://doi.org/10.5194/amt-7-3917-
- 587 2014.
- 588 Lackmann GM (2002) Cold-Frontal Potential Vorticity Maxima, the Low-Level Jet, and Moisture
- Transport in Extratropical Cyclones. *Monthly Weather Review* 130 (1): 59–74.
- 590 https://doi.org/10.1175/1520-0493(2002)130<0059:CFPVMT>2.0.CO;2.
- 591 Lenaerts JTM, Camron MD, Wyburn-Powell CR and Kay JE (2020) Present-day and future
- 592 Greenland Ice Sheet precipitation frequency from CloudSat observations and the Community
- 593 Earth System Model. *The Cryosphere*, 14(7): 2253–2265. https://doi.org/10.5194/tc-14-2253-
- 594 202.
- Kattelmann RC (1997) Flooding from rain-on-snow events in the Sierra Nevada. *Destructive*
- 596 Water: Water-Caused Natural Disasters, Their Abatement and Control. International Association
- 597 of Hydrological Sciences.
- 598 McCabe GJ, Clark MP and Hay LE (2007) Rain-on-Snow Events in the Western United States.
- 599 Bulletin of the American Meteorological Society 88 (3): 319–28. https://doi.org/10.1175/BAMS-
- 600 88-3-319.
- 601 McCrystall MR, Stroeve J, Serreze M, Forbes BC and Screen JA (2021) New Climate Models
- Reveal Faster and Larger Increases in Arctic Precipitation than Previously Projected. *Nature*
- 603 Communications 12 (1): 6765. https://doi.org/10.1038/s41467-021-27031-y.
- Niwano M and 5 others (2021) Rainfall on the Greenland ice sheet: present-day climatology
- from a high-resolution non-hydrostatic polar regional climate model. Geophysical Research
- 606 Letters, 48(15), e2021GL092942. https://doi.org/10.1029/2021GL092942.
- Nunatsiaq News (2021) Mild stretch sets the stage for record-breaking warmth in Iqaluit.
- Nunatsiaq News. https://nunatsiaq.com/stories/article/mild-stretch-sets-the-stage-for-record-
- 609 breaking-warmth-in-iqaluit/.
- Pan CG, Kirchner PB, Kimball JS, Kim Y and Du J (2018) Rain-on-Snow Events in Alaska, Their
- Frequency and Distribution from Satellite Observations. *Environmental Research Letters* 13 (7):
- 612 075004. https://doi.org/10.1088/1748-9326/aac9d3.
- Putkonen J and Roe G (2003) Rain-on-Snow Events Impact Soil Temperatures and Affect
- 614 Ungulate Survival. Geophysical Research Letters 30 (4).
- 615 https://doi.org/10.1029/2002GL016326.
- Ralph FM and 6 others (2017) Atmospheric Rivers Emerge as a Global Science and
- 617 Applications Focus. Bulletin of the American Meteorological Society 98 (9): 1969–73.
- 618 https://doi.org/10.1175/BAMS-D-16-0262.1.
- 619 Ralph FM, Neiman PJ and Rotunno R (2005) Dropsonde Observations in Low-Level Jets over
- the Northeastern Pacific Ocean from CALJET-1998 and PACJET-2001: Mean Vertical-Profile
- and Atmospheric-River Characteristics. *Monthly Weather Review* 133 (4): 889–910.
- 622 https://doi.org/10.1175/MWR2896.1.
- Rauber RM, Olthoff LS, Ramamurthy MK and Kunkel KE (2000) The Relative Importance of
- Warm Rain and Melting Processes in Freezing Precipitation Events. *Journal of Applied*

- 625 Meteorology and Climatology 39 (7): 1185–95. https://doi.org/10.1175/1520-
- 626 0450(2000)039<1185:TRIOWR>2.0.CO;2.
- Rennert KJ, Roe G, Putkonen J and Bitz CM. (2009) Soil Thermal and Ecological Impacts of
- Rain on Snow Events in the Circumpolar Arctic. *Journal of Climate* 22 (9): 2302–15.
- 629 https://doi.org/10.1175/2008JCLI2117.1.
- Rutz JJ, Steenburgh WJ and Ralph FM (2014) Climatological Characteristics of Atmospheric
- Rivers and Their Inland Penetration over the Western United States. *Monthly Weather Review*
- 632 142 (2): 905–21. https://doi.org/10.1175/MWR-D-13-00168.1.
- 633 Semmens KA, Ramage J, Bartsch A and Liston GE (2013) "Early Snowmelt Events: Detection,
- 634 Distribution, and Significance in a Major Sub-Arctic Watershed" 8 (1): 014020.
- 635 https://doi.org/10.1088/1748-9326/8/1/014020.
- 636 Serreze MC, Crawford AD and Barrett AP (2015) Extreme Daily Precipitation Events at
- 637 Spitsbergen, an Arctic Island. *International Journal of Climatology* 35 (15): 4574–88.
- 638 https://doi.org/10.1002/joc.4308.
- 639 Serreze MC and others (2021) Arctic Rain on Snow Events: Bridging Observations to
- 640 Understand Environmental and Livelihood Impacts. Environmental Research Letters 16 (10):
- 641 105009. https://doi.org/10.1088/1748-9326/ac269b.
- 642 Serreze MC and 5 others (2022) Characteristics of Extreme Daily Precipitation Events over the
- 643 Canadian Arctic. *International Journal of Climatology* 42: 10353-10372.
- 644 https://doi.org/10.0002/joc.7907.
- Singh P, Spitzbart G, Hübl H and Weinmeister, HW (1997) Hydrological Response of Snowpack
- under Rain-on-Snow Events: A Field Study. *Journal of Hydrology* 202 (1): 1–20.
- 647 https://doi.org/10.1016/S0022-1694(97)00004-8.
- 648 Trubilowicz JW and Moore RD (2017) Quantifying the Role of the Snowpack in Generating
- Water Available for Run-off during Rain-on-Snow Events from Snow Pillow Records.
- 650 *Hydrological Processes* 31 (23): 4136–50. https://doi.org/10.1002/hyp.11310.
- Voveris JJ (2022) Meteorological Drivers of Arctic Rain-on-Snow Events and How Climate
- 652 Change May Influence Associated Risks (Order No. 29069573). Available from Dissertations &
- Theses @ University of Colorado, Boulder; Dissertations & Theses @ University of Colorado
- 654 System; ProQuest Dissertations & Theses A&I; ProQuest Dissertations & Theses Global.
- 655 (2681751208). Retrieved from https://colorado.idm.oclc.org/login
- 656 Woollings T and 8 others (2018) Blocking and Its Response to Climate Change. Current Climate
- 657 Change Reports 4 (3): 287–300. https://doi.org/10.1007/s40641-018-0108-z.
- 658 Zhou Y and 5 others (2021) Uncertainties in Atmospheric River Lifecycles by Detection
- 659 Algorithms: Climatology and Variability. *Journal of Geophysical Research: Atmospheres* 126 (8):
- e2020JD033711. https://doi.org/10.1029/2020JD033711.